Optical ON/OFF Switching of Intramolecular Photoinduced Charge Separation in a Donor−Bridge−Acceptor System Containing Dithienylethene

Jochen M. Endtner,[†] Franz Effenberger,*[,†] Achim Hartschuh,[‡] and Helmut Port[‡]

Contribution from the Institut für Organische Chemie, Universität Stuttgart, Pfaffenwaldring 55, D-70569 Stuttgart, Germany, and 3. Physikalisches Institut, Universität Stuttgart, Pfaffenwaldring 57, D-70550 Stuttgart, Germany

Received November 1, 1999. Revised Manuscript Received January 26, 2000

Abstract: In the newly designed photoswitchable electron transfer compound **2**, our previously published donor−bridge−acceptor system (anthracene−CH_2−bithiophene−pyridinium) is modified by incorporation of the photoisomerizable dithienylethene (DTE) as a switching unit. In the open-ring form **2a**, excitation of the anthracene donor leads to an intramolecular charge separation proved by identification of the anthracene radical cation in transient absorption spectra (ON state). After photocyclization to the closed-ring isomer (**2a** → **2b**), the intramolecular charge separation is completely suppressed (OFF state). The reversibility of the ON/OFF switching is verified. From UV−vis absorption spectra and cyclovoltammetric studies it is deduced that in the open-ring isomer **2a** (ON state) conjugation is markedly restricted within the dithienylethene bridge, whereas in the closed-ring isomer **2b** (OFF state) the conjugation is extended over the whole dithienylethenepyridinium (DTEP) subunit. Consequently, in **2** an enlarged conjugation within the bridge is not decisive for photoinduced charge separation. Instead the observed transfer properties can be understood by thermodynamic aspects.

Introduction

The design of molecular photonic devices is a challenging subject of contemporary chemistry with respect to applications in molecular-scale information processing systems[1] and biomimetic engineering.[2]

In an approach to molecular-scaled devices we have intensively studied photoinduced intramolecular electron[3] and energy transfer processes[4] in bridged donor−acceptor (D−B−A) systems. With the intention to realize switchable transfer systems our investigations have mainly dealt with the influence of structural factors such as distance, orientation, and electronic interactions between donor and acceptor on appearance and dynamics of transfer processes. Thus we have already developed a D−B−A system with ON/OFF photoswitchable intramolecular *energy* transfer by incorporation of a photochromic fulgimide between anthracene and coumarin.[5]

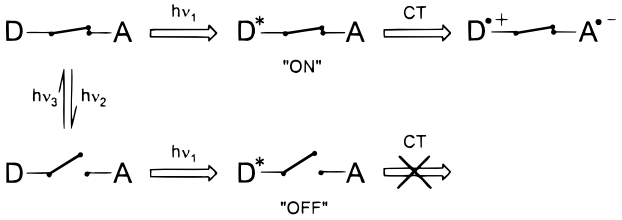

Figure 1. Schematic illustration of the photoswitchable intramolecular photoinduced charge separation (CT) with D as electron donor and A as acceptor.

In this paper we are concerned with the results of a D−B−A system which we have designed for optical control of photoinduced *electron* transfer. As depicted in Figure 1, the D−B−A system should comply with the following features: (i) In the ON state of the D−B−A system a photoexcitation at $h\nu_1$ results in a complete intramolecular electron transfer (CT) from the donor (D) to the acceptor (A), whereas after excitation ($h\nu_1$) of the D−B−A system in the OFF state, no charge separation occurs. (ii) Both forms, the ON and the OFF state, are thermally stable. (iii) The photoinduced transformation between the ON and the OFF state ($h\nu_2$ and $h\nu_3$, respectively) is achieved by a photoisomerizable unit, which is part of the bridge (B). (iv) The transformation is reversible.

In the literature, several systems concerning "photoswitchable electron transfer" have been described. In a sense similar to the concept of Figure 1, Tsuchiya presented a D−A system based on azobenzene-linked diporphyrin Zn complexes, which in the photochemically generated cis isomer indicates an

[†] Institut für Organische Chemie.

[‡] 3. Physikalisches Institut.

(1) (a) Lehn, J.-M. *Supramolecular Chemistry*; VCH: Weinheim, 1995; Chapter 8, pp 89−138. (b) Balzani, V.; Scandola, F. *Supramolecular Photochemistry*; Ellis Horwood: New York, 1991; Chapter 12, pp 355−394. (c) Ashwell, G. J. *Molecular Electronics*; Research Studies Press: Taunton, Somerset, 1992.

(2) (a) Kurreck, H.; Huber, M. *Angew. Chem.* **1995**, *107*, 929−947; *Angew. Chem., Int. Ed. Engl.* **1995**, *34*, 849−866. (b) Gust, D. *Nature* **1997**, *386*, 21−22 and references therein.

(3) (a) Hartschuh, A.; Port, H.; Wolf, H. C.; Miehlich, B.; Endtner, J. M.; Vollmer, M. S.; Effenberger, F. *J. Lumin.* **1998**, *76* and *77*, 655−657. (b) Hirsch, T.; Port, H.; Wolf, H. C.; Miehlich, B.; Effenberger, F. *J. Phys. Chem.* **1997**, *B101*, 4525−4535.

(4) (a) Vollmer, M. S.; Effenberger, F.; Stümpfig, T.; Hartschuh, A.; Port, H.; Wolf, H. C. *J. Org. Chem.* **1998**, *63*, 5080−5087. (b) Vollmer, M. S.; Würthner, F.; Effenberger, F.; Emele, P.; Meyer, D. U.; Stümpfig, T.; Port, H.; Wolf, H. C. *Chem.−Eur. J.* **1998**, *4*, 260−269. (c) Würthner, F.; Vollmer, M. S.; Effenberger, F.; Emele, P.; Meyer, D. U.; Port, H.; Wolf, H. C. *J. Am. Chem. Soc.* **1995**, *117*, 8090−8099.

(5) (a) Walz, J.; Ulrich, K.; Port, H.; Wolf, H. C.; Wonner, J.; Effenberger, F. *Chem. Phys. Lett.* **1993**, *213*, 321−324. (b) Port, H.; Hennrich, M.; Seibold, M.; Wolf, H. C. *Proc.−Electrochem. Soc.* **1998**, *98−25* (Excitonic Processes in Condensed Matter), 61−70.

10.1021/ja9938736 CCC: $19.00
Published on Web 03/14/2000

Chart 1. Photoisomerization of Newly Designed Systems **1** and **2** and Known Compound **3**[9]

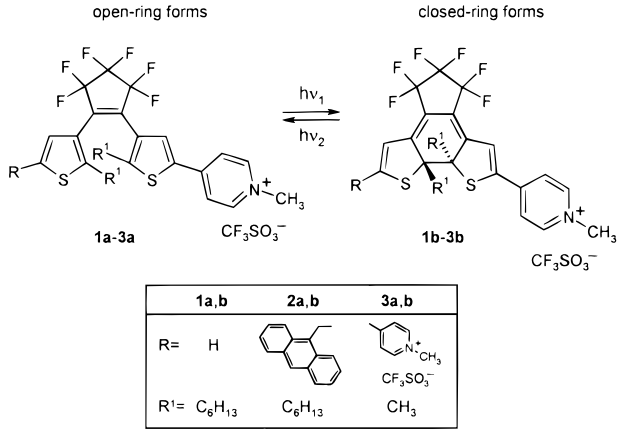

intramolecular electron transfer (ON state). The ON state, however, is thermally unstable and isomerizes back to the trans form (OFF state) within 1 h in the dark.[6] The experiments on a $D_1-A_1-A_2-D_2$ system described by Wasielewski et al.[7] have objectives different from those depicted in Figure 1. In this system photoinduced formation of $D_1^+-A_1^-$ or $A_2^--D_2^+$ is inhibited by the presence of an electric field initiated on a picosecond time scale by photogeneration of the adjacent radical ion pair.

The term "photoswitchable electron transfer" is also used for photoswitching the degree of conjugation in a symmetrically substituted bridge.[8,9] In ref 8, a system is studied with two ruthenium (Ru) metal centers connected by a dicyanonorbornadiene bridge. The two forms of the system, before and after photoinduced change in conjugation, exhibit different electronic interactions between the metal centers when oxidized to the Ru(II)−Ru(III) state. In ref 9, the system **3a** (Chart 1) comprises two electroactive pyridinium substituents connected via a dithienylethene (DTE) bridge. The photoconversion of DTE results in modified redox potentials of the substituents.

In our previous work on photoinduced electron transfer, the donor anthracene was linked to the acceptor pyridinium via a conjugated π-system made up of bithiophene or of differently sized polyenes.[3,10] Electronic interactions between donor and acceptor were systematically varied by incorporation of a methylene σ-spacer between anthracene and the conjugated bridge and by variation of the linkage position at the pyridinium, respectively. The occurrence of charge separation was proved by identification of the anthracene radical cation in transient absorption. For model compounds with a methylene spacer it was shown that intramolecular charge separation occurs independently of type and length of the conjugated π-system only in the case of para linkage at pyridinium. This result demonstrated that minor structural changes between donor and acceptor allow an interruption of the photoinduced electron transfer.[3,11] In the next step, maintaining the donor−spacer unit and 4-pyridinium acceptor, the conjugated bridge is replaced by photochromic DTE,[12] whose structure and conjugation properties can reversibly be varied by light between a state favorable and another one unfavorable for electron transfer. The decision to use a DTE bridge as a photochromic unit was made due to its excellent and well-studied chemical and physical properties,[12,13] maintained upon substitution.[9,14]

In the present publication we report on the synthesis of the DTE-bridged donor−acceptor triad **2** (Chart 1) as well as on spectroscopic and electrochemical properties of the two isomeric forms **2a** and **2b**, providing evidence for photoswitchable charge transfer in accordance with our concept in Figure 1.

Results and Discussion

Synthesis. The synthetic route for the preparation of molecules **2a** and **12a**, illustrated in Scheme 1, is based on the building-block principle, which involves the preparation of both molecular units **9a** and **10** required as reference compounds for physical investigations. *n*-Hexyl chains were linked to the DTE unit in order to enhance solubility.[15]

2-Hexylthiophene (**5**), the starting material for the preparation of the known DTE derivative **6**,[15] has been obtained in 73% yield from 2-lithiothiophene[16] and hexyl bromide. Compound **6** was prepared according to the methodology developed by Lehn et al.[15] To obtain **6** in high purity additional bulb-to-bulb distillation and repeated chromatography was necessary. By these purification steps compound **6** was isolated in 27% yield with 94% GC purity. Due to difficult chromatographic separation of the impurities, we have developed another purification method: **6** was reacted with triisopropylchlorosilane to yield the 2-fold triisopropylsilyl-substituted derivative **8**, which can readily be isolated either by chromatography or due to its excellent crystallization properties. **8** was obtained as colorless crystals, whose structure was determined by X-ray analysis.[17] The silyl group could be removed by addition of a 3.5-fold excess of trifluoromethanesulfonic acid to a solution of **8** in CCl_4 at −20 °C. After filtration through silica gel, **6** was isolated almost quantitatively as a colorless oil with 99% GC purity. Comparable yield and purity have been achieved using $NBu_4F\cdot 3H_2O$ in diethyl ether[18] as the desilylation agent for **8** (see Experimental Section).

The donor-substituted dyad unit **10** has been prepared from **6** by a two-step procedure. First, **6** dissolved in THF was lithiated with BuLi in hexane at −20 °C, and subsequently the thienyllithium intermediate was reacted with 9-anthracenecarbaldehyde to give the diarylcarbinol **7** in 55% yield.

Analogously to a method developed for benzyl and dibenzyl alcohols,[19] the diarylcarbinol **7** was reduced with sodium cyanoborohydride ($NaBH_3CN$) and zinc iodide to give compound **10** as a high-viscosity yellow oil in 74% yield. The instability of the molecular unit **10**, which has to be stored at

(6) Tsuchiya, S. *J. Am. Chem. Soc.* **1999**, *121*, 48−53.
(7) Gosztola, D.; Niemczyk, M. P.; Wasielewski, M. R. *J. Am. Chem. Soc.* **1998**, *120*, 5118−5119.
(8) Lainé, P.; Marvaud, V.; Gourdon, A.; Launay, J.-P.; Argazzi, R.; Bignozzi, C.-A. *Inorg. Chem.* **1996**, *35*, 711−714.
(9) Gilat, S. L.; Kawai, S. H.; Lehn, J.-M. *Chem.—Eur. J.* **1995**, *1*, 275−284.
(10) Effenberger, F.; Niesert, C.-P. *Synthesis* **1992**, 1137−1144.
(11) Effenberger, F.; Miehlich, B.; Endtner, J. M.; Vollmer, M. S.; Münter, J. S. R.; Hartschuh, A.; Lehle, J.; Port, H.; Wolf, H. C. Publication in preparation.
(12) (a) Irie, M.; Mohri, M. *J. Org. Chem.* **1988**, *53*, 803−808. (b) Hanazawa, M.; Sumiya, R.; Horikawa, Y.; Irie, M. *J. Chem. Soc., Chem. Commun.* **1992**, 206−207.
(13) Irie, M.; Uchida, K. *Bull. Chem. Soc. Jpn.* **1998**, *71*, 985−996.
(14) (a) Fernández-Acebes, A.; Lehn, J.-M. *Adv. Mater.* **1998**, *10*, 1519−1522. (b) Tsivgoulis, G. M.; Lehn, J.-M. *Adv. Mater.* **1997**, *9*, 39−42. (c) Kawai, S. H.; Gilat, S. L.; Ponsinet, R.; Lehn, J.-M. *Chem.—Eur. J.* **1995**, *1*, 285−293. (d) Irie, M.; Eriguchi, T.; Takada, T.; Uchida, K. *Tetrahedron* **1997**, *53*, 12263−12271. (e) Bens, A. T.; Frewert, D.; Kodatis, K.; Kryschi, C.; Martin, H.-D.; Trommsdorff, H. P. *Eur. J. Org. Chem.* **1998**, 2333−2338.
(15) Tsivgoulis, G. M.; Lehn, J.-M. *Chem.—Eur. J.* **1996**, *2*, 1399−1406.
(16) Brandsma, L.; Verkruijsse, H. D. *Preparative Polar Organometallic Chemistry 1*; Springer: Berlin, 1987; p 124.
(17) Endtner, J. Dissertation in preparation, Universität Stuttgart.
(18) Davies, S. G.; Goodfellow, C. L. *Synlett* **1989**, 59−62.
(19) Lau, C. K.; Dufresne, C.; Bélanger, P. C.; Piétré, S.; Scheigetz, J. *J. Org. Chem.* **1986**, *51*, 3038−3043.

Scheme 1[a]

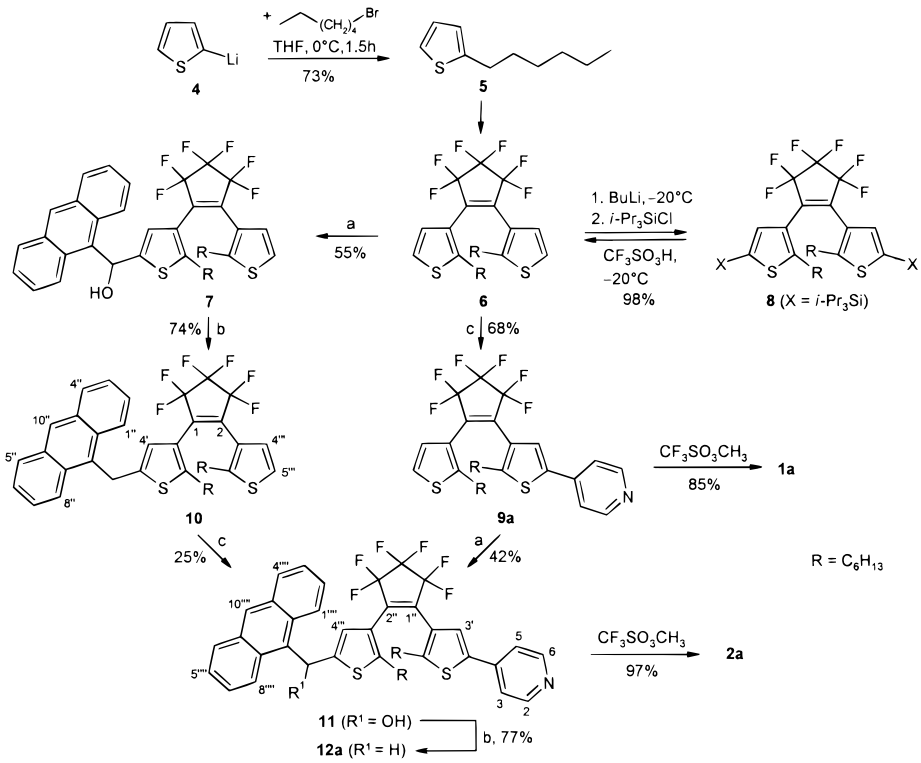

[a] Reaction conditions: (a) (1) *n*-BuLi, THF, −20 or −45 °C, (2) 9-anthracenecarbaldehyde; (b) $NaBH_3CN$, ZnI_2, $ClCH_2CH_2Cl$ (DCE), 80 or 30 °C, according to ref 19; (c) (1) *n*-BuLi, THF, −30 °C; (2) $B(OBu)_3$, 1.5 h, (3) 4-bromopyridinium hydrochloride, dioxane or DME, 1 M aqueous Na_2CO_3 solution, $Pd(PPh_3)_4$, 65−70 °C.

−30 °C under an argon atmosphere, could be ascribed to the unsubstituted α-position in thiophene.[20]

The acceptor-substituted dyad **9a** was also prepared starting from **6**. The direct linkage of pyridine to **6** was reached by a Suzuki cross-coupling reaction.[21] Since boronic acids of dithienylethenes are known to be extremely unstable,[15] an in situ Suzuki coupling was performed: **6** was lithiated with BuLi in hexane at −30 °C and subsequently treated with butyl borate. The resulting thiopheneboronic acid intermediate was added to a mixture of 4-bromopyridine, which was generated from the corresponding hydrochloride with aqueous Na_2CO_3 solution, and the $Pd(PPh_3)_4$ catalyst in dioxane. To avoid disubstitution, an excess of **6** (referred to BuLi) was used. In this way compound **9a** could be obtained in 68% yield with >99% purity. Unreacted **6** was reisolated by chromatography.

Two synthetic pathways, starting either from **9a** or from **10**, open the approach to the desired compound **12a** (Scheme 1). Analogously to the procedure described for the preparation of **9a**, pyridine was introduced in the donor-substituted DTE derivative **10** via an in situ Suzuki coupling reaction to give **12a**. The low yield of 25% is due to the required intensive purification steps: **12a** was isolated as a high-viscosity oil, which was first enriched to 95% by MPLC followed by ultrapurification to >99.9% by HPLC (see Experimental Section).

The second route, linkage of the anthrylmethyl group, starts from pyridine derivative **9a**. Lithiation of thiophene in the presence of pyridine, however, is complicated by the possible nucleophilic addition of organolithium compounds to pyridine.[22] Under the applied reaction conditions (lithiation at −45 °C in THF/hexane) **9a** was converted with 9-anthracenecarbaldehyde to the carbinol **11** in 42% yield. Reduction of **11** with $NaBH_3CN/ZnI_2$ gave **12a** in 77% yield (96% purity) after simple chromatography on silica gel.

9a and **12a** were methylated using methyl trifluoromethanesulfonate in diethyl ether. Chromatographic purification gave the pyridinium salt **1a** in 85% yield and **2a** as a yellow solid in 97% yield with >99% purity.

1a and **2a** were photoisomerized to **1b** and **2b** by irradiation at given wavenumbers (see Experimental Section, Table 2). In the case of dyad **1a**, a quantitative cyclization was reached. Upon photocyclization of **2a**, the solution contains only 87% of **2b** besides 13% of **2a** in the photostationary state.

Molecular Modeling. The optimized structures of open- and closed-ring isomers **2a**/**2b** obtained by molecular modeling[23] are depicted in Figure 2.

From Figure 2a it can be seen that in the force field the thiophene rings in **2a** arrange in an antiparallel conformation. As in the cyclized isomer **2b** (Figure 2b), the distance between anthracene and pyridinium (centers of gravity) amounts to 12 Å. The flexibility of the open-ring DTE in **2a**, however, allows in principle also a conformation in which both molecular groups can approach up to a minimum distance of 4 Å.

Photophysical Properties: Absorption Spectra. Absorption spectra of dyads **1** and triads **2** are analyzed successively in order to follow up the maintenance of photochromism and the

(20) Tsivgoulis, G. M.; Lehn, J.-M. *Adv. Mater.* **1997**, *9*, 627−630.

(21) (a) Miyaura, N.; Suzuki, A. *Chem. Rev.* **1995**, *95*, 2457−2483. (b) Martin, A. R.; Yang, Y. *Acta Chem. Scand.* **1993**, *47*, 221−230. (c) Miyaura, N.; Yanagi, T.; Suzuki, A. *Synth. Commun.* **1981**, *11*, 513−519. (d) Miyaura, N.; Yamada, K.; Suginome, H.; Suzuki, A. *J. Am. Chem. Soc.* **1985**, *107*, 972−980. (e) Zhang, H.; Kwong, F. Y.; Tian, Y.; Chan, K. S. *J. Org. Chem.* **1998**, *63*, 6886−6890.

(22) (a) Vollmer, M. S. Dissertation, Universität Stuttgart, 1996. (b) Spitzner, D. In *Houben Weyl, Methoden der Organischen Chemie*, 4th ed.; Kreher, R. P., Ed.; Thieme: Stuttgart, 1992; Vol. E7b, Part 2, pp 678−680 and references therein.

(23) BIOSYM Insight II, Discover 95.0/3.00, CVFF Force field.

Table 1. Absorption Maxima $\tilde{\nu}_{max}$ and Extinction Coefficients ϵ in Acetonitrile at 20 °C

compd	$\tilde{\nu}_{max}$/cm^{-1} (ϵ/M^{-1} cm^{-1})
A−CH_3[a]	26000 (9000), 27400 (9100), 28800 (5700), 39200 (217000)
9a	34800 (2100), 41000 (18700)
9b[b]	17500 (8000), 28000 (6800), 38000 (14800)
1a	28350 (26300), 42400 (17500)
1b	15500 (10700), 24800 (8300), 35000 (20100)
3a[c]	28400 (46000)
3b[c]	15100 (16000)
12a	25850 (9200), 27200 (9900), 28700 (7100), 33300 (19000), 39200 (128000)
12b[b]	17000 (9200), 25900 (12700), 27200 (14300), 28600 (9700), 39200 (130800)
2a	25850 (10500), 27300 (26600), 28600 (28900), 39200 (117200)
2b	15400 (11250), 24700 (8300),[d] 25800 (13000), 27200 (10400), 28700 (6900), 35200 (17700), 39200 (118300)

[a] In hexane, data from the literature.[27] [b] Respective closed-ring isomers of **9a** and **12a** (Scheme 1). [c] Data from the literature.[9] [d] Shoulder.

Table 2. Photoinduced Isomerization from Open to Closed Forms

solvent	wavenumber (cm^{-1})	open → closed (%)[a]
hexane/EtOAc = 9:1	32300	**9a** → **9b** (70 ± 5)
hexane/EtOAc = 55:45	28600	**12a** → **12b** (25)[b]
CH_3CN	28500 or 28100	**1a** → **1b** (99)
CH_3CN	28500	**2a** → **2b** (87 ± 5)

[a] Amount in the photostationary state at room temperature. [b] **12b** was enriched to 70% by MPLC (hexane/EtOAc = 55:45, 25 mL/min) and isolated by preparative HPLC (hexane/EtOAc = 85:15, 20 mL/min, 258 nm detection wavelength): 4 mg (8%) as a black blue solid.

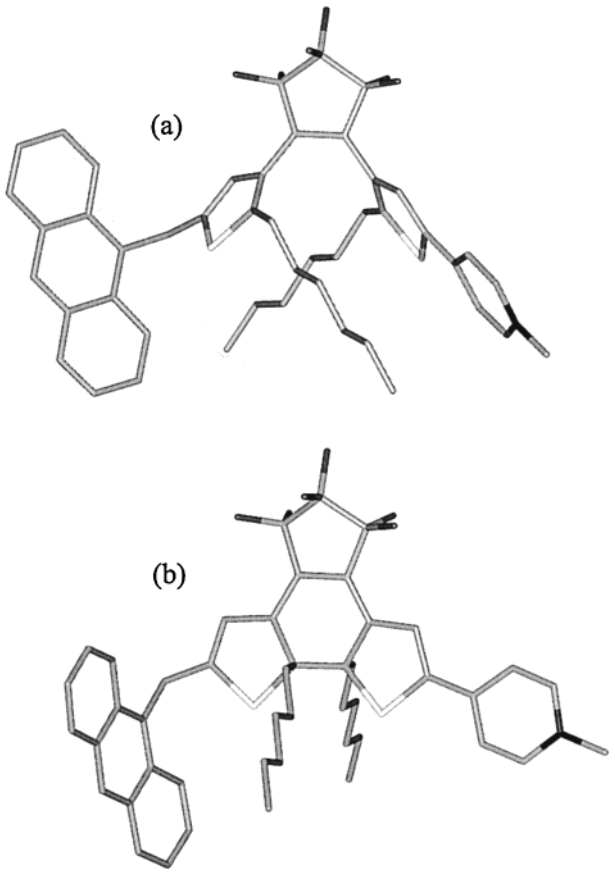

Figure 2. Structure of **2** obtained by molecular modeling: (a) open-ring triad **2a**; (b) closed-ring triad **2b**.

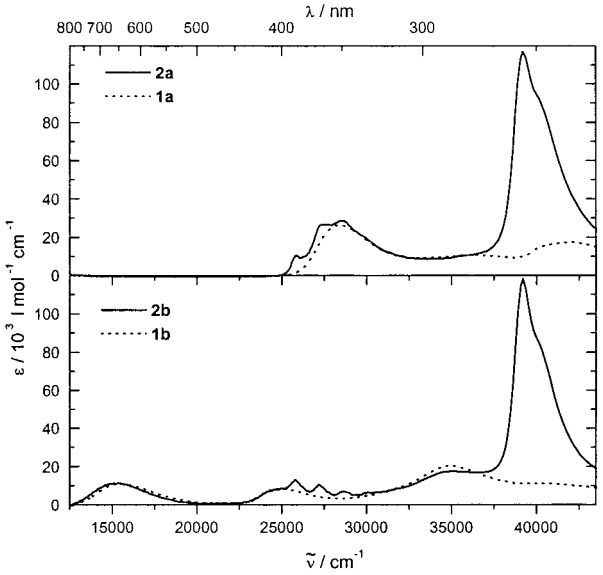

Figure 3. UV−vis absorption spectra (CH_3CN, T = 293 K) of open isomers **1a** and **2a** (top) and their closed forms **1b** and **2b** (bottom). The absorption spectrum of **2b** displayed was calculated on the basis of the spectrum of the isomeric mixture in the photostationary state with consideration of ^{1}H NMR and HPLC−UV−vis data.

coupling effects between the molecular subunits (Figure 3, top, and Table 1).

Open-ring dyad **1a** shows a sequence of unstructured absorption bands in the range above 25 000 cm^{-1} with a low-energy maximum at 28 350 cm^{-1}. Compound **3a**[9,15] (Chart 1) containing two thienylpyridinium units exhibits a similar absorption maximum with an extinction coefficient roughly twice as high as that of **1a**. The absorption at 28 350 cm^{-1} therefore must be assigned to the thienylpyridinium unit which both compounds have in common. The identification of this unit shows the effective electronic decoupling of the two thienyl components in the open-ring DTE in **1a** and **3a**. Hence, a conjugation through the open-ring DTE in **1a** can be excluded.

Cyclization of **1a** to **1b** leads to a drastic bathochromic shift of the absorption band to 15500 cm^{-1} (Figure 3, bottom), indicating improved π-orbital overlap and therefore large extension of conjugation in the closed-ring isomer.[14b,24,25a,b]

An important prerequisite for complete photoisomerization is separated absorption bands in the open and the closed form. This prerequisite is largely fulfilled in the case of isomers **1a**/**1b**. For photocyclization of **1a** to **1b** the solution was irradiated at 28600 cm^{-1}, where the absorption maximum of **1a** coincides with a minimum in **1b**. In functionalized dithienylethenes the quantum yield for cyclization is much higher than for ring

(24) Saika, T.; Irie, M.; Shimidzu, T. *J. Chem. Soc., Chem. Commun.* **1994**, 2123−2124.

(25) (a) Knoll, K.; Schrock, R. R. *J. Am. Chem. Soc.* **1989**, *111*, 7989−8004. (b) Brédas, J. L.; Silbey, R.; Boudreaux, D. S.; Chance, R. R. *J. Am. Chem. Soc.* **1983**, *105*, 6555−6559. (c) Kiehl, A.; Eberhardt, A.; Adam, M.; Enkelmann, V.; Müllen, K. *Angew. Chem.* **1992**, *104*, 1623−1626; *Angew. Chem., Int. Ed. Engl.* **1992**, *31*, 1588−1591.

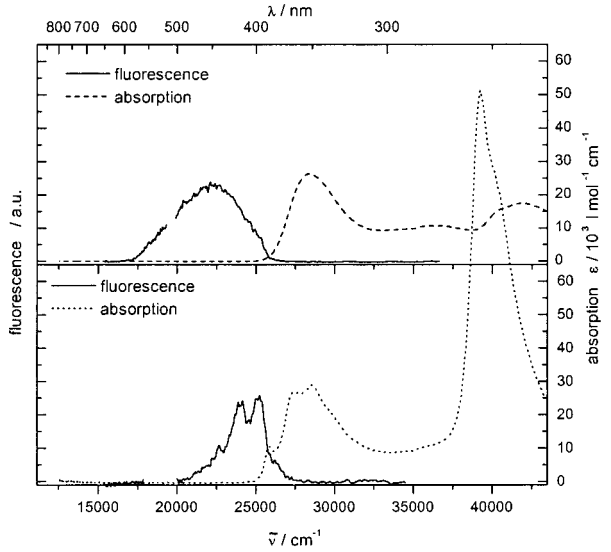

Figure 4. Fluorescence spectra (CH_3CN, T = 293 K) of open chromophores after excitation at 39200 cm^{-1}: (top) dyad **1a**; (bottom) triad **2a** (au = arbitrary units; signals at 19600 cm^{-1} originate from the second order of excitation light and are omitted).

opening (bleaching),[9,14d,e,26] so that at 28600 cm^{-1} excitation ring opening plays a minor role compared with the cyclization. On the contrary, closed **1b** can be bleached quantitatively at wavenumbers above 20000 cm^{-1} even if the quantum yield is low. This is owing to its low energetic absorption band completely separated from the absorption of **1a**.

Concerning the absorption spectra of triads **2a**/**2b** we focused our interest on how the methylene spacer-decoupled anthracene donor influences the spectroscopic behavior of the dithienylethenepyridinium unit. A comparison of the absorption spectra of triads **2a** and **2b** (Figure 3, Table 1) with that of 9-methylanthracene[27] demonstrates that the anthracene-type absorption between 43500 and 38500 cm^{-1} and in the range 33500−25000 cm^{-1} remains independent of the isomerization of the DTEP subunit. As can be seen from Figure 3, the absorption bands of triad **2a**/**2b** originate from a superposition of anthracene and the respective dyad **1a**/**1b**, even though in **2a**/**2b** the typical anthracene S_0-S_3 band at 39200 cm^{-1} is slightly broadened and less intensive than in 9-methylanthracene.[27] Inversely, the DTEP units also preserve their individuality in triad **2a**/**2b** so that the characteristic conjugation and photoisomerization properties of the dyads essentially are maintained in the triads.

Thus the spectra of triads **2a**/**2b** can be interpreted completely by superposition of anthracene and DTEP. Additional absorption bands due to mixed states or direct CT transition are not observed. The spectroscopic coexistence of anthracene and DTEP chromophores reveals that both units are effectively decoupled by the methylene spacer. This allows one to address individually either one of these chromophores. The relative excitation probability at a given wavelength (excitation selectivity) depends on the respective extinction coefficients.

Fluorescence Spectra. Figure 4 shows the fluorescence spectra of the open-ring isomers **1a** and **2a** after excitation at 39200 cm^{-1}.

The spectrum of the open-ring dyad **1a** exhibits a broad structureless fluorescence band with a maximum at 22200 cm^{-1} (Figure 4, top). Attachment of the anthrylmethyl group in **2a** induces a completely different fluorescence spectrum with a maximum at 24700 cm^{-1}. Due to its spectral shape and vibrational structure the fluorescence band of **2a** (Figure 4, bottom) can be assigned to the anthracene S_1 emission.[28] Upon changing the excitation to 28600 cm^{-1}, where the anthracene contribution to the total absorption is rather small (<10% in contrast to 90% at 39200 cm^{-1}), the fluorescence spectrum of **2a** maintains its anthracene-type shape.

The closed-ring forms of both dyad **1b** and triad **2b** display no fluorescence in the examined spectral range (11100−25000 cm^{-1}), indicating complete quenching of the anthracene fluorescence.

Electrochemical Properties. Redox potentials allow one to assess the *relative energy positions* of the frontier orbitals (HOMO and LUMO) of isolated or electronically decoupled molecular units.[29] Therefore electrochemical measurements contribute in combination with the optical investigations, from which the HOMO−LUMO *gaps* can be obtained, to understand the energetics of intramolecular processes.

Energetically low-lying HOMOs (high ionization potential) lead to high anodic (positive) oxidation potentials, while energetically high HOMOs exhibit less anodic potentials. The same argument applies to the LUMO energies and the reduction potentials: low-lying LUMOs (high electron affinity) lead to less cathodic (negative) reduction potentials, while high LUMOs require high cathodic potentials to effect electron uptake. In triad **2a**/**2b** the frontier orbitals (HOMO and LUMO) of anthracene and DTEP subunits can be regarded as being independent of each other owing to the effective electronic decoupling by the methylene spacer (compare UV−vis absorption spectra).

The electrochemical properties of **2a**,**b** were investigated by cyclic voltammetry (CV)[30] in acetonitrile at room temperature (0.1 M $Bu_4N^+PF_6^-$, scan rate = 1.0 V s^{-1}) as depicted in Figure 5.

Figure 5 (top) shows that the molecule in its open-ring form (**2a**) undergoes an irreversible oxidation process at +0.92 V. This process is assigned to an anthracene oxidation owing to the agreement with literature data of anthracene (+0.96 V)[31] and our investigations on similar compounds with anthracene donors (+0.92 and +0.94 V)[11] (all potentials vs ferrocene as internal standard).[32] In the examined potential range (up to +1.15 V) no oxidation of the DTEP subunit is observed, which is a typical finding for open-ring DTE derivatives as reported in the literature.[15,24] According to ref 25 high oxidation potentials correspond to short conjugation length. The deduced high oxidation potential of the DTEP subunit in **2a** therefore confirms the poor overlap of π-orbitals in the open-ring form, becoming apparent in the UV−vis absorption spectra. The less anodic oxidation of anthracene compared to that of the DTEP subunit indicates that the anthracene HOMO in **2a** is energetically higher than the HOMO of the DTEP subunit.

In the cathodic range a reversible process occurs at −1.54 V which according to literature data[33] corresponds to the reduction

(26) Irie, M.; Sakemura, K.; Okinaka, M.; Uchida, K. *J. Org. Chem.* **1995**, *60*, 8305−8309.

(27) (a) Würthner, F. Dissertation, Universität Stuttgart, 1993. (b) Steiner, R. P.; Michl, J. *J. Am. Chem. Soc.* **1978**, *100*, 6861−6867.

(28) Sawicki, E.; Hauser, T. R.; Stanley, T. W. *Int. J. Air Pollut.* **1960**, *2*, 253−272.

(29) (a) Kaim, W.; Ernst, S.; Kohlmann, S. *Chem. Unserer Zeit* **1987**, *21*, 50−58. (b) Lever, A. B. P. *Inorganic Electronic Spectroscopy*; Elsevier: Amsterdam, 1984. (c) Scherer, O. J.; Schwalb, J.; Swarowsky, H.; Wolmershäuser, G.; Kaim, W.; Gross, R. *Chem. Ber.* **1988**, *121*, 443−449.

(30) Heinze, J. *Angew. Chem.* **1984**, *96*, 823−840; *Angew. Chem., Int. Ed. Engl.* **1984**, *23*, 831−848.

(31) Wallis, J. M.; Kochi, J. K. *J. Am. Chem. Soc.* **1988**, *110*, 8207−8223.

(32) Beck, F. *Elektroorganische Chemie: Grundlagen und Anwendungen*; Verlag Chemie: Weinheim, 1974; pp 103 and 208.

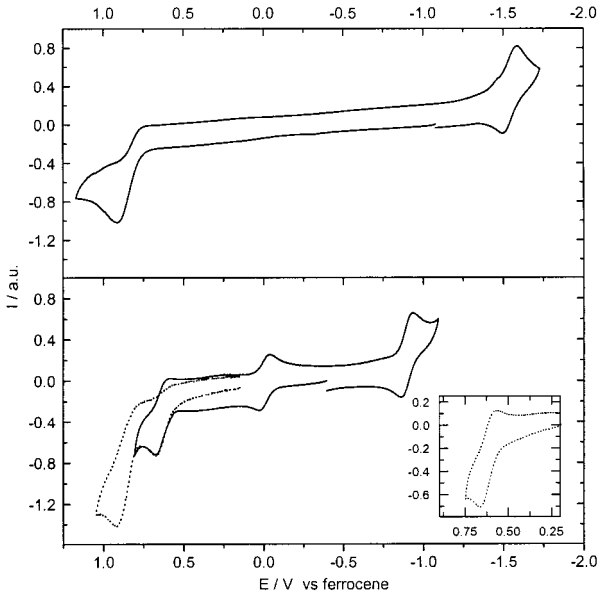

Figure 5. Cyclic voltammograms of the triad **2** (CH_3CN, 0.1 M $Bu_4N^+PF_6^-$; scan rate $\upsilon = 1.0$ V s^{-1}): (top) open-ring form **2a**; (bottom) closed-ring form **2b**. The potential peak at 0 V is related to ferrocene as internal reference. Inset: first oxidation peak of **2b** at scan rate $\upsilon =$ 2.0 V s^{-1}.

of the pyridinium group. The resulting unpaired electron on the pyridinium unit is stabilized by the adjacent thiophene ring. As a consequence the reversibility of the electrode process is enhanced.[11]

The CV curves of the closed-ring triad **2b** are shown in Figure 5 (bottom). As in **2a** the spacer-decoupled anthracene is irreversibly oxidized at a peak potential of +0.92 V, but in contrast to **2a** an additional, partially reversible oxidation at +0.62 V is observed. The clearly facilitated release of electrons in the closed-ring isomer **2b** can be attributed to an increased conjugation.[24,25] The concomitant stabilization of the generated radical cation also explains the partial reversibility of this electrode process. It is noteworthy that, in contrast to **2a**, the HOMO in the closed-ring form **2b** is localized on the DTEP subunit.

In its closed-ring form **2b**, the molecule shows a cathodic reduction already at −0.89 V. The considerable lowering of the LUMO within the DTEP dyad upon cyclization may be related to electron-withdrawing effects of the CF_2 groups.[9]

In both isomers **2a**,**b** the DTEP subunit is reduced first, indicating that its LUMOs are energetically lower than the respective LUMO of anthracene.

Transient Absorption Spectra. Figure 6 shows the transient absorption spectra of a complete switching cycle (open → closed → open form) of triad **2a**/**2b** recorded 7 ps after laser pulse excitation at 25850 cm^{-1}.

Figure 6 (top) presents the transient absorption spectrum of open-ring form **2a** in comparison with the anthracene radical cation of 9-methylanthracene[34] and the transient absorption of dyad **1a**. A structured signal with maxima at 14500, 15800, and 17400 cm^{-1} dominates the spectrum of **2a**. As can be seen from Figure 6 (top), the vibronic structure of **2a** corresponds well with that of the anthracene radical cation. At 17400 cm^{-1} the radical cation band is overlapped by a transient absorption due to the DTEP subunit which can be explained by direct excitation of the DTEP subunit (15% of total absorption at

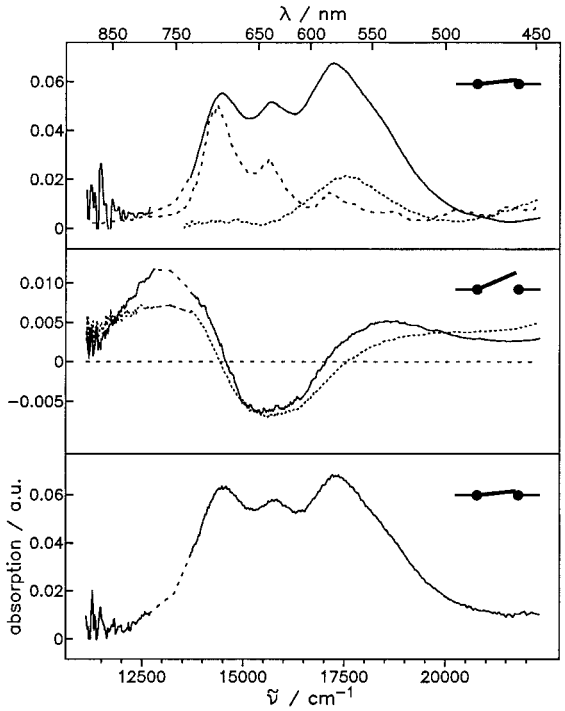

Figure 6. Transient absorption of an ON−OFF−ON switching cycle of **2a**/**2b** (2.8×10^{-4} M in CH_3CN, $T = 293$ K) recorded 7 ps after laser pulse excitation at 25850 cm^{-1}: (top) triad **2a** (—), dyad **1a** (···), and anthracene radical cation of 9-methylanthracene[34] (- - -); (middle) **2b** in the photostationary state after irradiation at 28600 cm^{-1} (—), and **1b** (···); (bottom) spectrum after bleaching of the solution of **2b** at 18950 cm^{-1}. Signals at 12900 cm^{-1} were extrapolated (distortion due to suppression of the laser fundamental).

25850 cm^{-1}). The appearance of the anthracene radical cation in the open-ring triad **2a** is unequivocal evidence for an intramolecular electron transfer with anthracene as the donor. Additional investigations of the excited state dynamics indicate that the charge-separated state (D^+-A^-) originates from a neutral state of the photoexcited anthracene donor (D*−A).[35]

After photocyclization of the sample solution (**2a** → **2b**) by irradiation at 28600 cm^{-1}, the transient absorption spectrum changes completely (Figure 6, middle). The spectra of the closed-ring forms of triad **2b** and dyad **1b** are nearly identical with absorption contributions below 14500 cm^{-1} and above 17000 cm^{-1}, and a negative signal between due to bleaching of ground state absorption. No anthracene-type radical cation $D^{+\bullet}$ is observed, although the selectivity of anthracene excitation in **2b** amounts to ca. 45% at 25850 cm^{-1}. The absence of $D^{+\bullet}$ reveals that an intramolecular electron transfer in the closed-ring form **2b** can be excluded. Also no indication for a photoexcited anthracene donor (D*) becomes apparent in further investigations of the excited state dynamics for the closed-ring isomer **2b**.[35]

After photoinduced reopening (**2b** → **2a**) upon irradiation at 18950 cm^{-1} the transient absorption spectrum of **2a** is recovered (Figure 6, bottom). Thus the reversibility of switching is verified.

The transient absorption spectroscopic results show that by a primary externally triggered process (photoisomerization of DTE) a secondary externally initiated process (intramolecular photoinduced electron transfer) can be converted by light reversibly between the ON and the OFF state. Thus in the case of triad **2a**/**2b** the term "photoswitchable photoinduced electron transfer" is justified.

(33) Pragst, F.; Santrucek, M. *J. Prakt. Chem.* **1987**, *329*, 67−80.

(34) Shida, T. *Electronic absorption spectra of radical ions* (*Physical sciences data 34*); Elsevier: Amsterdam, 1988.

(35) Hartschuh, A. Dissertation in preparation, Universität Stuttgart.

Discussion of the Photoswitchable Electron Transfer in 2a/2b. The photoinduced electron transfer (CT) only occurs in the open-ring form **2a** (ON state), in which the conjugation within the DTE bridge is markedly restricted. Conversely, no charge separation is possible in the closed-ring form **2b** (OFF state), in which the conjugation within the DTEP subunit is fully extended. These results demonstrate that in triad **2a**/**2b** improved conjugation within the DTE bridge is not decisive for an intramolecular photoinduced electron transfer. The model of a "conjugation switch" in the sense of photoswitchable "molecular wire" [14b,24,36] therefore cannot be transferred to our compounds. In this context it must be considered that, contrary to **2a**, the anthracene−pyridinium distance in the rigid closed-ring form **2b** is fixed (12 Å). Hence, the spatial conditions (rigidity/distance) in **2b** correspond with those of our previously described triad system anthracene−CH_2−bithiophene−4-pyridinium,[3a] in which, in contrast to **2b**, complete charge separation has been proved. Therefore the donor−acceptor distance is also not a decisive criterion for electron transfer in **2a**/**2b**.

Thermodynamic aspects are fundamental for the occurrence of photoinduced charge separation. Relevant parameters for **2a**/**2b** are discussed by simplified molecular orbital diagrams derived by the following considerations: (i) Anthracene and the DTEP subunit are spectroscopically and electrochemically decoupled by the methylene spacer, and thus the frontier orbitals (HOMO/LUMO) of the units can be regarded independent of each other. (ii) The gap between HOMO and LUMO corresponds to the $E_{0.0}$ transition of the respective molecular unit. The HOMO−LUMO gap determined from the optical $E_{0.0}$ transition may differ from that determined from electrochemical data.[29] This difference, however, is neglected in our discussion. (iii) The relative energy position of HOMOs and LUMOs results from the oxidation and reduction potential, respectively. To estimate the HOMO energy of the anthracene unit of **2a**/**2b** the anodic peak potential of anthracene oxidation (+0.92 V) was used as the approximate value.

All physical investigations were performed under identical experimental conditions (solvent, temperature) so that data can be compared directly with each other. The $E_{0.0}$ transition of the anthracene unit (A−CH_2) was determined from the average of fluorescence and absorption maxima of **2a** (Figure 4, bottom) to be 25630 cm^{-1} ≙ 3.18 eV.[37] The $E_{0.0}$ transition of the open DTEP unit was deduced analogously from the spectra of dyad **1a** (Figure 4, top) (25400 cm^{-1} ≙ 3.15 eV), while that of the closed DTEP unit was derived from the difference of the corresponding redox potentials of **2b** (1.51 eV ≙ 12180 cm^{-1}), since no emission could be detected in this case. It is noteworthy that the potential for the reduction of the anthracene unit (−2.26 V) obtained by summing up the $E_{0.0}$ transition and the approximate HOMO energy of anthracene is in good agreement with literature data.[38]

The resulting relative energy positions of the frontier orbitals of anthracene and the DTEP subunit in **2a**/**2b** are illustrated in Figure 7.

The application of orbital energies on intramolecular electron transfer of **2a** starting from locally excited anthracene is shown in Figure 8 (left side). Using our experimental values in the Rehm−Weller equation[39] ignoring the Coulomb term,[40] the free energy change $\Delta G_{CT(a)}$ for the photoinduced electron transfer is determined to be −0.72 eV, and thus definitely exergonic. The occurrence of photoinduced charge separation in the open-ring triad **2a** is therefore thermodynamically justified. In the closed-ring triad **2b** no photoinduced charge separation occurs, although the free energy change for electron transfer originating from locally excited anthracene (Figure 8, right side) is exergonic as well ($\Delta G_{CT(b)}$ = −1.37 eV). Obviously after anthracene excitation, in **2b** an additional intramolecular process occurs, suppressing a possible electron transfer.

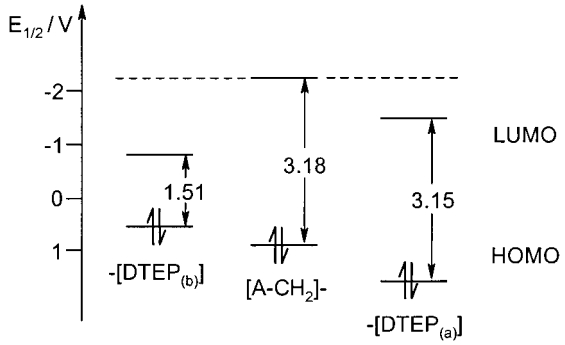

Figure 7. Molecular orbital diagram of frontier orbitals of anthracene and DTEP unit in triad **2**. The scale is referred to the redox potentials vs ferrocene. The distance between HOMO and LUMO corresponds with the $E_{0.0}$ transition given in eV.

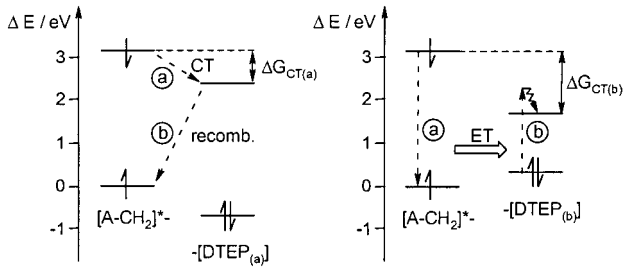

Figure 8. Illustration of intramolecular transfer processes in **2** after local excitation of the anthracene donor [A−CH_2], considering the orbital energies from Figure 7: (left) intramolecular electron transfer (CT) in **2a**; (right) intramolecular energy transfer (ET) in **2b**.

As was mentioned above, the transient absorption spectrum of **2b** (Figure 6, middle) closely resembles the spectrum of dyad **1b**. A quantitative evaluation of transient absorption spectra of **1b** and **2b** (excitation at 25850 cm^{-1})[41] yields comparable relative signal intensities for both compounds, although the DTEP subunit in **2b** contributes to the total absorption only 55%. This means that in the case of anthracene excitation in **2b** a quantitative energy relaxation (energy transfer) to the DTEP subunit occurs as illustrated in Figure 8 (right side). The quenching of anthracene fluorescence in **2b** is in line with this conclusion.

Energy transfer (ET) and electron transfer (CT) are thermodynamically controlled pathways. The probability for either process being operative depends to a large extent on the overall free energy changes.[40] The molecular orbital diagram of **2b** (Figure 8, right side) allows one to compare the free energy changes of charge separation ($\Delta G_{CT(b)}$) and energy transfer ($\Delta G_{ET(b)}$): Owing to the extremely low energy transitions of the closed-ring DTEP subunit, the energy transfer in **2b** ($\Delta G_{ET(b)}$ = −1.67 eV)[42] is significantly more exergonic than a possible electron transfer ($\Delta G_{CT(b)}$ = −1.37 eV). According to this

(36) (a) Larsson, S.; Braga, M. *Chem. Phys.* **1993**, *176*, 367−375. (b) Joachim, C.; Launay, J. P.; Woitellier, S. *Chem. Phys.* **1990**, *147*, 131−141.
(37) Ephardt, H.; Fromherz, P. *J. Phys. Chem.* **1991**, *95*, 6792−6797.
(38) Anowski, S.; Voss, J. *J. Prakt. Chem.* **1996**, *338*, 337−344.
(39) Rehm, D.; Weller, A. *Isr. J. Chem.* **1970**, *8*, 259−271.
(40) Kavarnos, G. J.; Turro, N. J. *Chem. Rev.* **1986**, *86*, 401−449.
(41) Hartschuh, A.; Endtner, J. M. Unpublished results.
(42) The free energy change for the energy transfer ΔG_{ET} was estimated from the difference of the respective $E_{0.0}$ transitions.

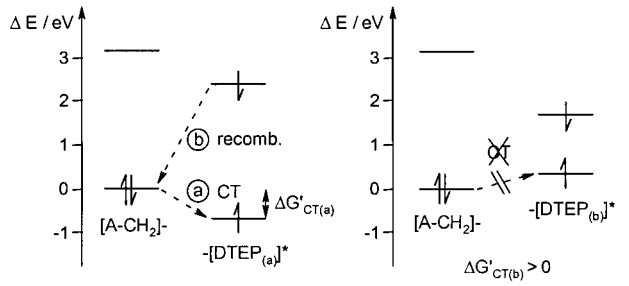

Figure 9. Illustration of intramolecular electron transfer (CT) in **2a** (left), and forbidden intramolecular electron transfer in **2b** (right) after excitation of the DTEP subunit [$DTEP_{(a)}$] and [$DTEP_{(b)}$], respectively.

molecular orbital diagram, the energy transfer clearly represents the energetically preferred process ($\Delta G_{ET(b)} < \Delta G_{CT(b)}$).

Conversely, in the open-ring triad **2a** an energy transfer, competitive to the observed charge separation, is not to be expected from an energetic point of view (Figure 8, left side). In this case, the free energy change for energy transfer ($\Delta G_{ET(a)}$)[42] is close to zero due to comparable $E_{0.0}$ transitions of anthracene and the DTEP subunit. Therefore energy transfer in **2a** is clearly less exergonic than electron transfer ($\Delta G_{CT(a)} \ll \Delta G_{ET(a)}$).

In the preceding section the thermodynamic aspects for the case of photoexcitation of the anthracene donor in **2a**/**2b** have been considered. The experimental conditions, however, partly involve direct excitation of the DTEP subunits. Therefore the thermodynamic arguments for charge separation after local excitation of the DTEP subunits in **2a**/**2b** have to be discussed as well (Figure 9).

Taking the experimentally determined energy positions for open-ring triad **2a** illustrated in Figure 9 (left side), an electron transfer originating from photoexcited DTEP is found exergonic ($\Delta G'_{CT(a)} = -0.69$ eV) and thus thermodynamically preferred against an energy transfer between DTEP and anthracene ($\Delta G'_{CT(a)} \ll \Delta G'_{ET(a)}$). For such a charge transfer, however, there is no experimental evidence.

In contrast to **2a**, in closed-ring triad **2b** a charge separation by optical excitation of the DTEP subunit would be endergonic, since in **2b** the HOMO of the DTEP subunit is energetically higher than that of the anthracene donor (see Figure 9, right side). Consequently, charge separation is not allowed thermodynamically in **2b**.

In summary, the presented electron transfer properties of **2** are in accord with thermodynamic arguments, demonstrating the importance of thermodynamic factors in deciding on the dominating intramolecular transfer processes.

Conclusion

On the basis of our previous work on structurally controlled intramolecular photoinduced transfer processes, we have designed a novel dithienylethene-bridged donor−acceptor compound **2b** which is capable of reversibly ON/OFF photoswitchable (photoinduced) charge separation (Figure 1). The photoactive DTE bridge, directly attached to the pyridinium acceptor, is separated from the anthracene donor by incorporation of a methylene σ-spacer. Therefore both the donor and the switch−acceptor subunit maintain their spectroscopic identity and can be addressed individually by light. In the open-ring isomer **2a** excitation of the donor results in an intramolecular charge separation identified by the anthracene radical cation (ON state). In the photocyclized closed-ring isomer **2b** no charge separation occurs (OFF state). Obviously improved conjugation within the bridge is not decisive for the charge separation in **2**, so that in this case the DTE unit does not function like the "conjugation switch" anticipated and widely discussed in the literature.

Experimental Section

General Methods. Melting points were determined on a Büchi SMP 20 apparatus and are uncorrected. ^{1}H NMR spectra were recorded on a Bruker AC 250 F (250 MHz) or a Bruker ARX 500 (500 MHz) instrument. Chemical shifts are given in parts per million relative to tetramethylsilane as internal standard. Preparative column chromatography was performed on silica gel S, grain size 0.032−0.063 mm (Riedel-de Haen). Medium-pressure liquid chromatography (MPLC) was carried out at 10 bar using a 50 × 4 cm LiChroPrep Si60 (15−20 μm) column (Merck). Analytical HPLC was performed using either an ET 200/4 Nucleosil 100-5 column (Macherey Nagel), flow 1 mL/min, hexane/ EtOAc = 90:10 or 92:8, or an ET200/8/4 Nucleosil 100-5 C_{18} AB column (Macherey Nagel), flow 1 mL/min, MeOH/MeCN/CH_2Cl_2 = 50:40:10. Preparative HPLC was performed using a 250 × 32 mm LiChrosorb Si60 5 μm column (Knauer). The purity was determined by gas chromatography using a Hewlett-Packard series II 5890 with FID, 0.6 bar of hydrogen, 20 m capillary column, phase OV 1701. UV−vis spectra were recorded on a Perkin-Elmer Lambda 7 photospectrometer with quartz cuvette (d = 1 cm). Fast-atom bombardment (FAB) mass spectra were obtained using a NBA matrix. For the photoinduced isomerization a XBO 75 W lamp (Osram) or a krypton ion laser was applied.

All solvents were purified and dried. All reactions were performed in flame-dried glassware under an inert gas atmosphere.

Transient Absorption Measurement. A 2.8×10^{-4} M solution of the respective chromophore **1a**/**1b** or **2a**/**2b** in MeCN (ca. 25 mL) was pumped continuously through a flow cell (0.45 cm thickness). In a storage vessel, integrated in the cycle, the solution is regenerated by irradiation with unfocused laser light. All sub-picosecond transient absorption spectra were monitored with a white-light continuum after pulse excitation at 25850 cm^{-1}. For details on the experimental setup refer to the literature.[3b,43]

2-Hexylthiophene (5). To a solution of thiophene (122.1 g, 1.45 mol) in THF (320 mL) at −10 °C under Ar was added a 1.6 M solution of BuLi in hexane (605 mL, 0.97 mol) dropwise over 1.5 h. After being stirred for a further 1.5 h at room temperature, the reaction mixture was cooled to 0 °C, and a solution of hexyl bromide (159.7 g, 0.97 mol) in THF (100 mL) was added dropwise over 1 h. The reaction mixture was stirred at room temperature for 15 h, hydrolyzed with water, and extracted with Et_2O. The combined extracts were washed with water and dried (Na_2SO_4). Solvent and unreacted thiophene were removed, and the residue was distilled through a Vigreux column to give 118.5 g (73%) of **5** as a colorless liquid: bp 92 °C/10 Torr (114 °C/14 Torr[44]); ^{1}H NMR (250 MHz, $CDCl_3$) δ 0.89 (t, J = 6.6 Hz, 3H, CH_3), 1.31 (m, 6H, 3 CH_2), 1.67 (m, 2H, CH_2), 2.81 (t, J = 7.9 Hz, 2H, CH_2), 6.77 (m, 1H, H3), 6.91 (dd, J = 5.1, 3.4 Hz, 1H, H4), 7.08 (dd, J = 1.2 Hz, 1H, H5).

1,2-Bis(2′-hexylthiophene-3′-yl)perfluorocyclopentene (6).[15] **6** was prepared in a procedure analogous to that described in the literature;[15] however, bulb-to-bulb distillation (120−150 °C/0.001 Torr) and repeated chromatography on silica gel with hexane was required to obtain **6** as a light yellow oil with 94% GC purity (27% yield).

Purification of 6 by Conversion to 1,2-Bis(2′-hexyl-5′-triisopropylsilylthien-3′-yl)perfluorocyclopentene (8). To a stirred solution of crude **6** (9.54 g, 60% GC purity) in absolute THF (80 mL) at −20 °C under Ar in the absence of light was added a 1.6 M solution of BuLi in hexane (24.0 mL, 38.4 mmol) dropwise (temperature kept at −20 °C), and the reaction mixture was stirred for a further 30−45 min. After dropwise addition of triisopropylchlorosilane (8.35 mL, 39.4 mmol), the reaction mixture was allowed to warm to room temperature (2 h), hydrolyzed with water, and extracted with Et_2O. The combined extracts were washed with water, dried (Na_2SO_4), and concentrated.

(43) Handschuh, M.; Seibold, M.; Port, H.; Wolf, H. C. *J. Phys. Chem.* **1997**, *A101*, 502−506.

(44) Buu-Hoï, Ng. Ph.; Lavit, D.; Xuong, Ng. D. *J. Chem. Soc.* **1955**, 1581−1583.

The residue was chromatographed on silica gel with hexane. Recrystallization from *i*-Pr_2O/MeOH (1:1) afforded 8.49 g (55% referred to crude **6**) of **8** as colorless crystals: mp 87.5 °C; ^{1}H NMR (500 MHz, $CDCl_3$) δ 0.84 (t, J = 7.1 Hz, 3H, CH_3), 1.08 (d, J = 7.4 Hz, 18H, $(CH_3)_2CH$), 1.12−1.25 (m, 6H, 3 CH_2), 1.29 (m, 3H, $(CH_3)_2CH$), 1.42 (m, 2H, CH_2), 2.16 (t, J = 7.8 Hz, 2H, CH_2), 7.14 (s, 1H, H4″). Anal. Calcd for $C_{43}H_{70}F_6S_2Si_2$: C, 62.88; H, 8.59; S, 7.81. Found: C, 62.92; H, 8.67; S, 7.94.

Removal of the TIPS Protecting Group. To a solution of **8** (6.16 g, 7.5 mmol) in absolute CCl_4 (400 mL) at −20 °C under Ar in the absence of light was added trifluoromethanesulfonic acid (2.32 mL, 26.6 mmol) dropwise by syringe, and the reaction mixture was stirred for 1 h. The reaction mixture was then filtered through silica gel with hexane to give 3.74 g (98%) of **6** as a colorless oil with >99% GC purity.

Alternatively, to a solution of **8** (0.22 g, 0.26 mmol) in Et_2O (15 mL) under Ar in the absence of light was added $NBu_4F{\cdot}3H_2O$ (0.32 g, 1.02 mmol). After being stirred at 33 °C for 5 h, the reaction mixture was filtered through a silica gel column with hexane, and the filtrate was concentrated to give 0.131 g (99%) of **6** as a colorless oil (GC purity >98%).

1-[5′-(9″-Anthrylhydroxymethyl)-2′-hexylthien-3′-yl]-2-(2‴-hexylthien-3‴-yl)perfluorocyclopentene (7). To a solution of **6** (2.13 g, 4.2 mmol) in THF (15 mL) at −20 °C under Ar in the absence of light was added a 1.6 M solution of BuLi in hexane (3.0 mL, 4.8 mmol) dropwise, and the reaction mixture was stirred at −5 °C for a further 40 min. A solution of anthracene-9-carbaldehyde (0.87 g, 4.2 mmol) in THF (25 mL) was added dropwise over 30 min. The reaction mixture was allowed to warm to room temperature (3.5 h), hydrolyzed with water, and extracted with Et_2O. The combined extracts were washed with water, dried (Na_2SO_4), and concentrated. The residue was chromatographed on silica gel with CH_2Cl_2/hexane (80:20). Fractions containing **7** and unreacted solid anthracenecarbaldehyde were mixed with a small volume of ice-cold EtOH. Anthracenecarbaldehyde was filtered off, and the filtrate was chromatographed to give totally 1.65 g (55%) of **7** as a yellow high-viscosity oil: ^{1}H NMR (500 MHz, $CDCl_3$) δ 0.77 (t, J = 7.3 Hz, 3H, CH_3), 0.85 (t, 3H, CH_3), 0.86−1.30 (m, interfered, 16H, 8 CH_2), 1.99 (m, 2H, CH_2), 2.16 (t, J = 7.8 Hz, 2H, CH_2), 2.81 (d, J = 4.0 Hz, 1H, OH), 6.50 (s, 1H, H4′), 6.90 (d, J = 5.3 Hz, 1H, H4‴), 7.06 (d, 1H, H5‴), 7.45−7.50 (m, 5H, H2″,3″,6″,7″, CH), 8.05 (m, 2H, H4″,5″), 8.41 (m, 2H, H1″,8″), 8.50 (s, 1H, H10″). Anal. Calcd for $C_{40}H_{40}F_6OS_2$: C, 67.21; H, 5.64; S, 8.97. Found: C, 66.91; H, 5.82; S, 8.61.

1-[5′-(9″-Anthrylmethyl)-2′-hexylthien-3′-yl]-2-(2‴-hexylthien-3‴-yl)perfluorocyclopentene (10). To a vigorously stirred solution of **7** (1.30 g, 1.8 mmol) in DCE (40 mL) at 60 °C under Ar in the absence of light was added a mixture of $NaBH_3CN$ (0.96 g, 15.3 mmol) and ZnI_2 (1.09 g, 3.4 mmol). After being stirred at 80 °C for 24 h, the reaction mixture was poured onto ice−water and acidified with concentrated HCl to dissolve the inorganic salts formed. After extraction with CH_2Cl_2, the combined extracts were washed with water until neutral and then were dried ($MgSO_4$). Concentration and chromatography on silica gel with hexane/CH_2Cl_2 (70:30) afforded 0.93 g (74%) of **10** as a yellow oil, which was stored under Ar at −30 °C: ^{1}H NMR (500 MHz, $CDCl_3$) δ 0.81 (m, 6H, CH_3), 0.87−1.25 (m, interfered, 16H, 8 CH_2), 1.99 (t, J = 7.7 Hz, 2H, CH_2), 2.05 (t, 2H, CH_2), 5.03 (s, 2H, CH_2), 6.65 (s, 1H, H4′), 6.93 (d, J = 5.4 Hz, 1H, H4‴), 7.07 (d, 1H, H5‴), 7.49 (m, 4H, H2″,3″,6″,7″), 8.03 (m, 2H, H4″,5″), 8.23 (m, 2H, H1″,8″), 8.43 (s, 1H, H10″). Anal. Calcd for $C_{40}H_{40}F_6S_2$: C, 68.74; H, 5.77; S, 9.18. Found: C, 68.62; H, 5.85; S, 9.12.

4-{4′-[2″-(2‴-Hexylthien-3‴-yl)perfluorocyclopenten-1″-yl]-5′-hexylthien-2′-yl}pyridine (9a). (a) Compound **6** (1.40 g, 2.75 mmol) in THF (45 mL) was lithiated at −30 °C as described above using a 1.6 M solution of BuLi in hexane (1.35 mL, 2.2 mmol). To the reaction mixture was quickly added butyl borate (1.2 mL, 4.5 mmol) by syringe. The cooling bath was removed, and the reaction mixture was stirred for 1.5 h.

(b) To solid 4-bromopyridinium hydrochloride (0.81 g, 4.2 mmol) in dioxane (30 mL) under Ar was added a 1 M aqueous Na_2CO_3 solution (20 mL) to generate 4-bromopyridine, and the suspension was heated to 50 °C. The catalyst $Pd(PPh_3)_4$ (48 mg, 0.04 mmol) was added followed by addition of the reaction mixture from part a by cannula. After being stirred at 65 °C for 2 h, the reaction mixture was hydrolyzed with ice−water and extracted with CH_2Cl_2. The combined extracts were washed with saturated NH_4Cl solution followed by water until neutral, dried (Na_2SO_4), and concentrated. The residue was chromatographed on silica gel with hexane/EtOAc (6:4) to give 0.87 g (68% referred to BuLi) of **9a** as a brownish yellow viscous oil with 99% GC purity: ^{1}H NMR (500 MHz, $CDCl_3$) δ 0.72 (t, J = 7.0 Hz, 3H, CH_3), 0.87 (t, J = 7.2 Hz, 3H, CH_3), 1.00−1.34 (m, interfered, 16H, 8 CH_2), 2.21 (t, J = 7.8 Hz, 2H, CH_2), 2.26 (t, J = 8.0 Hz, 2H, CH_2), 7.07 (dt, J = 5.4, 1.4 Hz, 1H, H4‴), 7.24 (dt, 1H, H5‴), 7.41 (dd, J = 4.5, 1.7 Hz, 2H, H3,5), 7.45 (t, J = 1.2 Hz, 1H, H3′), 8.60 (dd, 2H, H2,6); UV−vis data, see Table 1. Anal. Calcd for $C_{30}H_{33}F_6NS_2$: C, 61.52; H, 5.68; N, 2.39; S, 10.95. Found: C, 61.55; H, 5.76; N, 2.38; S, 11.02.

Fractions containing unreacted **6** were chromatographed on silica gel with hexane to reisolate 0.48 g (35%) of **6**.

4-{4′-[2″-(5‴-(9⁗-Anthrylhydroxymethyl)-2‴-hexylthien-3‴-yl)-perfluorocyclopenten-1″-yl]-5′-hexylthien-2′-yl}pyridine (11). To **9a** (0.10 g, 0.17 mmol) in hexane (1 mL) under Ar in the absence of light was added THF (3.2 mL), and the solution was cooled to −45 °C. A 1.6 M solution of BuLi in hexane (0.15 mL, 0.24 mmol) was slowly added by syringe. After the reaction mixture was stirred for 15 min, anthracenecarbaldehyde (38 mg, 0.18 mmol) was added over 1 min, and the reaction mixture was stirred for 1.5 h. The cooling bath was removed, and to the reaction mixture were added water (15 mL) and Et_2O (10 mL). The phases were separated, and the aqueous phase was extracted with Et_2O. The combined organic phases were washed with water until neutral, dried (Na_2SO_4), and concentrated. The residue was chromatographed on silica gel with hexane/EtOAc (6:4), and the product-containing fractions were filtered through $NaHCO_3$ to give 57 mg (42%) of **11** as a yellowish brown high-viscosity oil: ^{1}H NMR (500 MHz, $CDCl_3$) δ 0.76 (t, J = 7.9 Hz, 3H, CH_3), 0.80 (t, J = 7.2 Hz, 3H, CH_3), 0.88−1.36 (m, interfered, 16H, 8 CH_2), 2.00 (m, 2H, CH_2), 2.36 (t, J = 7.9 Hz, 2H, CH_2), 3.31 (br s, 1H, OH), 6.31 (s, 1H, H4‴), 7.18 (s, 1H, H3′), 7.23 (m, 2H, H3,5), 7.43−7.48 (m, 5H, H2⁗,3⁗,6⁗,7⁗, CH), 7.95 (m, 2H, H4⁗,5⁗), 8.34 (s, 1H, H10⁗), 8.39 (m, 2H, H1⁗,8⁗), 8.52 (m, 2H, H2,6). FAB-MS calcd for $C_{45}H_{43}F_6NOS_2$: 791.2690. Found: 791.2705.

Preparation of 4-{4′-[2″-(5‴-(9⁗-Anthrylmethyl)-2‴-hexylthien-3‴-yl)perfluorocyclopenten-1″-yl]-5′-hexylthien-2′-yl}pyridine (12a) from 11. To a solution of **11** (49 mg, 0.06 mmol) in DCE (7 mL) at 55 °C under Ar in the absence of light was added a mixture of $NaBH_3CN$ (0.13 g, 2.07 mmol) and ZnI_2 (0.127 g, 0.40 mmol) in two portions within 4 h. After being stirred at 30 °C for 24 h, the reaction mixture was filtered through a silica gel column with hexane/EtOAc (6:4). Product-containing fractions were concentrated and chromatographed on silica gel with hexane/EtOAc (6:4) to yield 36 mg (77%) of **12a** as a yellow oil (HPLC purity 96%): ^{1}H NMR (500 MHz, $CDCl_3$) δ 0.71 (t, J = 7.0 Hz, 3H, CH_3), 0.84 (t, J = 7.3 Hz, 3H, CH_3), 0.94−1.25 (m, interfered, 16H, 8 CH_2), 2.01 (t, J = 7.7 Hz, 2H, CH_2), 2.21 (t, J = 8.0 Hz, 2H, CH_2), 5.02 (s, 2H, CH_2), 6.52 (s, 1H, H4‴), 7.24 (s, 1H, H3′), 7.28 (d, J = 4.8 Hz, 2H, H3,5), 7.48 (m, 4H, H2⁗,3⁗,6⁗,7⁗), 7.99 (m, 2H, H4⁗,5⁗), 8.20 (m, 2H, H1⁗,8⁗), 8.34 (s, 1H, H10⁗), 8.57 (d, 2H, H2,6).

Preparation of 12a Starting from 10. 12a was prepared in a procedure analogous to that described above for the preparation of **9a**, using **10** (0.75 g, 1.1 mmol) in THF (20 mL), a 1.6 M solution of BuLi in hexane (1.0 mL, 1.6 mmol), butyl borate (0.6 mL, 2.2 mmol), 4-bromopyridinium hydrochloride (0.31 g, 1.6 mmol) in DME (30 mL), 1 M aqueous Na_2CO_3 solution (15 mL), and $Pd(PPh_3)_4$ (25 mg, 0.021 mmol), reaction time 3.5 h at 70 °C. Chromatography on silica gel with CH_2Cl_2/MeOH (96:4) and subsequently hexane/EtOAc (1:1) followed by ultrapurification by preparative HPLC (hexane/EtOAc = 85:15, 20 mL/min, 258 nm detection wavelength) gave 0.21 g (25%) of **12a** (HPLC purity >99.9%): ^{1}H NMR data correspond with those described above; UV−vis data, see Table 1. Anal. Calcd for $C_{45}H_{43}F_6NS_2$: C, 69.65; H, 5.59; N, 1.81; S, 8.26. Found: C, 69.83; H, 5.73; N, 1.67; S, 8.13.

General Procedure for the Preparation of Pyridinium Salts 1a, 2a. To a solution of **9a** (0.54 mmol) or **12a** (0.09 mmol) in Et_2O (8 mL (**9a**), 3.5 mL (**12a**)) at room temperature or 0 °C (**9a**) in the absence

of light was added freshly under Ar distilled methyl trifluoromethanesulfonate (ca. 1.2 equiv) dropwise by syringe. After being stirred for a further 30 min, the reaction mixture was filtered through a silica gel column with CH_2Cl_2/MeOH (90:10). Product-containing fractions were concentrated, taken up in a small volume of hexane/CH_2Cl_2 = 1:1 (**1a**) or 80:20 (**2a**), and filtered to remove silica gel.

4-{4′-[2″-(2‴-Hexylthien-3‴-yl)perfluorocyclopenten-1″-yl]-5′-hexylthien-2′-yl}-*N*-methylpyridinium trifluoromethanesulfonate (1a): colorless solid (85% yield); mp 118 °C; ^{1}H NMR (500 MHz, $CDCl_3$) δ 0.72 (t, J = 7.1 Hz, 3H, CH_3), 0.87 (t, J = 7.2 Hz, 3H, CH_3), 0.97−1.32 (m, interfered, 16H, 8 CH_2), 2.30 (m, 2H, CH_2), 2.32 (m, 2H, CH_2), 4.21 (s, 3H, NCH_3), 7.13 (d, J = 5.5 Hz, 1H, H4‴), 7.43 (d, 1H, H5‴), 8.03 (s, 1H, H3′), 8.07 (d, J = 6.9 Hz, 2H, H3,5), 8.51 (d, 2H, H2,6); UV−vis data, see Table 1. Anal. Calcd for $C_{32}H_{36}F_9NO_3S_3$: C, 51.26; H, 4.84; N, 1.87; S, 12.83. Found: C, 51.02; H, 4.79; N, 1.86; S, 12.74.

4-{4′-[2″-(5‴-(9⁗-Anthrylmethyl)-2‴-hexylthien-3‴-yl)perfluorocyclopenten-1″-yl]-5′-hexylthien-2′-yl}-*N*-methylpyridinium trifluoromethanesulfonate (2a): yellow solid (97% yield); mp 65 °C; HPLC purity >99%; ^{1}H NMR (500 MHz, $CDCl_3$) δ 0.72 (t, J = 7.0 Hz, 3H, CH_3), 0.82 (t, J = 7.3 Hz, 3H, CH_3), 0.95−1.18 (m, interfered, 16H, 8 CH_2), 2.08 (t, J = 7.6 Hz, 2H, CH_2), 2.34 (t, J = 7.8 Hz, 2H, CH_2), 4.23 (s, 3H, NCH_3), 5.04 (s, 2H, CH_2), 6.45 (s, 1H, H4‴), 7.51 (m, 4H, H2⁗,3⁗,6⁗,7⁗), 7.75 (s, 1H, H3′), 7.90 (d, J = 6.6 Hz, 2H, H3,5), 8.00 (m, 2H, H4⁗,5⁗), 8.25 (m, 2H, H1⁗,8⁗), 8.38 (s, 1H, H10⁗), 8.49 (d, 2H, H2,6); UV−vis data, see Table 1. FAB-MS calcd for $C_{46}H_{46}F_6NS_2$: 790.298. Found: 790.297.

Photoisomerization of Open-Ring Forms to Their Closed Isomers. A solution of open-ring form **1a**, **2a**, **9a**, or **12a** in the respective solvent (Table 2) was irradiated at the wavenumber given in Table 2 until the photostationary state was reached. The photostationary state was determined by HPLC and ^{1}H NMR spectroscopy and was controlled by UV−vis spectroscopy.

Acknowledgment. We thank Dr. B. Miehlich for molecular modeling studies and helpful discussions, Dr. R. F. Winter for cyclovoltammetric investigations, and Dr. A. Baro for assistance in preparing the manuscript.

JA9938736